

RECENT STUDIES OF BEAM PHYSICS FOR ION LINACS

L. Groening¹, S. Appel¹, M. Chung⁴, X. Du¹, P. Gerhard¹, M. Maier¹, S. Mickat¹,
 A. Rubin¹, P. Scharrer^{1,2,3}, H. Vormann¹, and C. Xiao¹

¹Gesellschaft für Schwerionenforschung, Darmstadt, Germany

²Helmholtz Institute Mainz, Mainz, Germany

³Johannes Gutenberg-University, Mainz, Germany

⁴Ulsan National Institute of Science and Technology, Ulsan 44919, Republic of Korea

Abstract

The UNiversal Linear ACcelerator (UNILAC) at GSI aims at provision of high brilliant heavy ion beams, as its main purpose will be to serve as injector for the upcoming FAIR accelerator complex. To keep acceleration efficient, heavy ions need to be charge state stripped and progress in improving this process is reported. Recent advance in modeling time-transition-factors and its impact on simulation of longitudinal dynamics is presented. The UNILAC injects into the subsequent synchrotron SIS18 applying horizontal multi-turn injection (MTI). Optimization of this process triggered intense theoretical and experimental studies of the dynamics of transversely coupled beams. These activities comprise full 4d transverse beam diagnostics, round-to-flat beam transformation, extension of Busch's theorem to accelerated particle beams, and optimization of the MTI parameters through generic algorithms.

INTRODUCTION

After being upgraded the UNILAC (Fig. 1) together with the subsequent synchrotron SIS18 will serve as injector for FAIR [1]. Three ion source terminals can be operated in pulse-to-pulse switching mode at 50 Hz. One terminal is equipped with an ECR source providing highly charged ions. Followed by an RFQ and an IH-cavity operated at 108 MHz it forms the High Charge Injector (HLI) providing beams at 1.4 MeV/u. Another terminal houses a Penning source (PIG) providing low intensity beams at intermediate charge states at 2.2 keV/u.

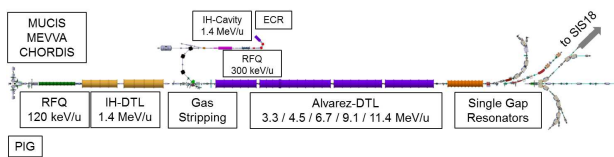


Figure 1: The upgraded UNiversal Linear ACcelerator (UNILAC) at GSI.

The third terminal is dedicated to provision of intense beams of low-charged ions at 2.2 keV/u as well. Intense heavy ion beams are produced in a MEVVA or VARIS. Beams are bunched and pre-accelerated to 120 keV/u along a 9 m long RFQ operated at 36 MHz. Afterwards two IH-cavities provide for acceleration to 1.4 MeV/u, being the exit energy of the High Current Injector (HSI). For uranium the highest particle numbers are obtained by using the charge

state $^{238}\text{U}^{4+}$. After the IH-DTL the acceleration efficiency is increased by passing the beam through a gaseous stripper which delivers the mean charge state of $^{238}\text{U}^{28+}$ at its exit. This increase of charge state is at the expense of intrinsic particle loss. Prior to 2014 about 87% of the uranium ions were stripped to charge states different from $^{238}\text{U}^{28+}$. After dispersive selection of the desired charge state the beam is matched to the subsequent post-stripper Alvarez-type DTL. The latter is operated at 108 MHz and comprises five tanks. Its exit beam energy is 11.4 MeV/u being the injection energy for the synchrotron SIS18. The post-stripper DTL can be fed with beams from the HLI as well. The design parameters to be achieved after the upgrade are listed in Table 1.

Table 1: Beam Design Parameters for the Upgraded UNILAC

Ion A/q	≤ 8.5	
Beam Current	1.76·A/q	mA
Input Beam Energy	1.4	MeV/u
Output Beam Energy	3.0 - 11.7	MeV/u
Emit. (norm., tot.) hor/ver	0.8/2.5	μm
Beam Pulse Length	≤ 1.0	ms
Beam Repetition Rate	10	Hz
Rf Frequency	108.408	MHz

This upgrade program is based on dedicated R&D w.r.t. the provision of high brilliant ion beams. It comprises the optimization of charge state stripping by passing the ion beam through a media as well as the improved modeling of longitudinal beam dynamics along DTL cavities. Diagnostics of the full 4-dimensional transverse phase space including inter-plane correlations was developed and successfully tested. A novel technique allows to transfer emittance from one transverse degree of freedom into the other one, thus increasing the efficiency of multi-turn injection. The modeling of this emittance shaping was simplified significantly by showing that the underlying dynamics are described by extending the Busch theorem from single particles to accelerated beams. Finally, generic algorithms were developed to optimize multi-turn injection into a synchrotron.

INCREASE OF STRIPPING EFFICIENCY

So far, a continuous N_2 jet has been used as stripping medium. The achieved stripping efficiency from $^{238}\text{U}^{4+}$ to $^{238}\text{U}^{28+}$ was 14%. Since 2014 a pulsed gas stripper cell has

been tested [2, 3]. It injects short gas pulses, the length of which matches the beam pulse length into the stripping chamber, producing a high density target without overloading the differential pumping system toward adjacent accelerator systems. Using H₂ the efficiency of stripping into the most populated charge state has been increased from 14% to 21%. Figure 2 compares measured charge state spectra of a uranium beam at 1.4 MeV/u applying a continuous N₂ jet with a spectrum resulting from a pulsed H₂ cell. The rms-width δq of the spectrum from the jet is about 3.6. The width from the pulsed cell is $\delta q \approx 2.3$, i.e. it is reduced by 36%. Another appealing feature of the pulsed stripper is its flexibility w.r.t. the applied back pressures of the single gas pulses as well as to the lengths of the individual pulses. Both can be changed in pulse-to-pulse switching mode of the UNILAC thus eliminating restrictions from the constant back pressure provided by the N₂ jet. Additionally, the set-up can be equipped with a second valve, thus allowing for pulse-to-pulse operation with a second stripper gas.

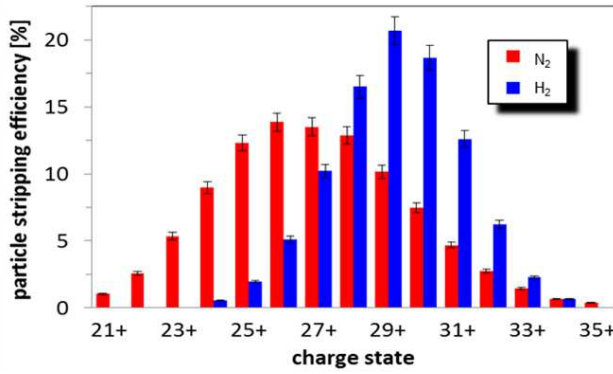


Figure 2: Comparison of measured uranium charge state spectra applying a continuous N₂ jet (red) with a spectrum resulting from a pulsed H₂ cell (blue).

Final optimization and implementation into routine operation of this new stripping set-up have started. A detailed description of the development and testing of the high pressure H₂ gas cell as well as the latest results obtained with the device are reported in [2, 3].

LONGITUDINAL MODELING OF DTLs

Any DTL cavity is a sequence of drifts and finite gaps. The dynamics inside gaps is quite demanding as the effective local forces on the beam particle are explicit functions of time and position. Usually, the equations are solved by doing the approximation that the particle velocity is constant during the gap transit. Although this approximation obviously contradicts to the purpose of gaps, namely increasing the velocity, it delivers reasonable results and generations of DTLs were designed in this way. To a huge fraction this is thanks to the focusing nature of the effective longitudinal lattice. Errors in velocities and rf-phases from that approximations cause oscillation around the design orbit even for the perfect particle. However, the errors are small and machine performance is not seriously harmed. This figure changes, if the

regular longitudinal focusing is weakened or partially abandoned as for the KONUS [4] beam dynamics that slightly moves attention from focusing towards efficiency of acceleration. The UNILAC pre-stripper DTL uses this dynamics for very efficient acceleration of ²³⁸U⁴⁺ and operation revealed that the longitudinal dynamics is very sensitive to small changes of cavity voltages and phases compared to the post-stripper DTL which uses Alvarez-type cavities.

In order to better understand these sensitivities the longitudinal modeling was refined as described in detail in [5]. The static electric field inside gaps is calculated by Fourier-Bessel series as implemented into the BEAMPATH code [6] using

$$E_z = -\cos(\omega t + \psi_0) \sum_{m=1}^M E_m I_0(\mu_m r) \sin\left(\frac{2\pi m z}{\Gamma}\right),$$

$$E_r = \cos(\omega t + \psi_0) \sum_{m=1}^M \frac{2\pi m E_m}{\mu_m \Gamma} I_1(\mu_m r) \cos\left(\frac{2\pi m z}{\Gamma}\right), \quad (1)$$

$$B_\theta = \sin(\omega t + \psi_0) \sum_{m=1}^M \frac{2\pi E_m}{\mu_m \lambda c} I_1(\mu_m r) \sin\left(\frac{2\pi m z}{\Gamma}\right),$$

and

$$\mu_m = \frac{2\pi}{\lambda} \sqrt{\left(\frac{m\lambda}{\Gamma}\right)^2 - 1}, \quad \Gamma = l + 2g + d,$$

$$E_m = \frac{4U}{I_0(\mu_m a)\Gamma} \frac{\pi m(l+g)}{\Gamma} \frac{\sin\left[\frac{\pi m(l+g)}{\Gamma}\right]}{\frac{\pi m(l+g)}{\Gamma}} \frac{\sin\left(\frac{\pi m g}{\Gamma}\right)}{\frac{\pi m g}{\Gamma}}, \quad (2)$$

where I_0 and I_1 are the Bessel functions of zero and first order, ω is the angular frequency of the field, r is the radial coordinate, U is the gap voltage, ψ_0 is the phase at the gap at $t=0$, and a, l, g, d define the gap geometry [5]. The single particle starts moving at $z=0$. Typically the number of Fourier harmonics is $M=30$. The reference particle vector function and its derivative w.r.t. z is defined as

$$Z(t, z) := \begin{bmatrix} z \\ \frac{dz}{dt} \end{bmatrix} = \begin{bmatrix} z \\ \beta c \end{bmatrix} \quad (3)$$

and

$$DZ(t, z) := \frac{dZ(t, z)}{dt} = \begin{bmatrix} \beta c \\ \frac{q}{m_0} E_z(z) \cos(\omega t + \psi_0) \end{bmatrix}. \quad (4)$$

This non-linear differential equation is solved by applying the Bulirsch-Stoer method. Using the refined modeling of a KONUS DTL the sensitivities mentioned above could be reproduced in simulations as reported in [5].

Additionally, the "intermediate" energy phenomenon of UNILAC's last two Alvarez-type cavities was finally modeled 35 years after it has been observed in operation. By chance it was found during commissioning of the fourth (fifth) DTL cavity, that it provides high quality beams with small energy spread, if it is operated just at 80% (70%) of its

Content from this work may be used under the terms of the CC BY 3.0 licence (© 2018). Any distribution of this work must maintain attribution to the author(s), title of the work, publisher, and DOI.

nominal voltage. The output energies are reduced by 34% (32%) compared to the nominal values. Although this was not understood, these beams are supplied to users since many decades to their full satisfaction. Using the advanced modeling these "intermediate" energies were exactly reproduced in simulations. Figure 3 shows the electric field strength along the DTL together with the respective reference particle energy. It reveals that the beam is even temporarily decelerated inside the cavity. The according longitudinal phase space distribution at the cavity exit is displayed in Fig. 4.

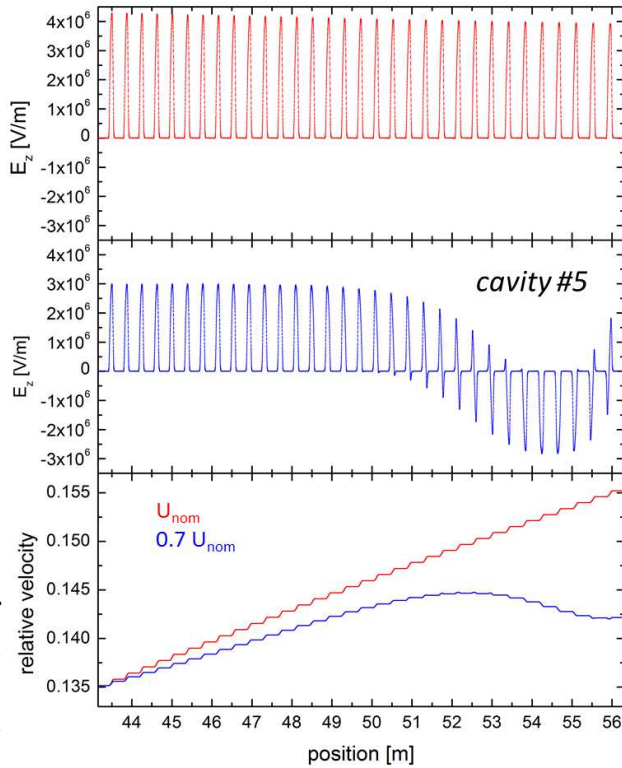


Figure 3: Longitudinal electric field strength as felt by the design particle at nominal cavity voltage (upper), at 70% of the nominal voltage (center), and the respective particle energies along the fifth DTL cavity (bottom).

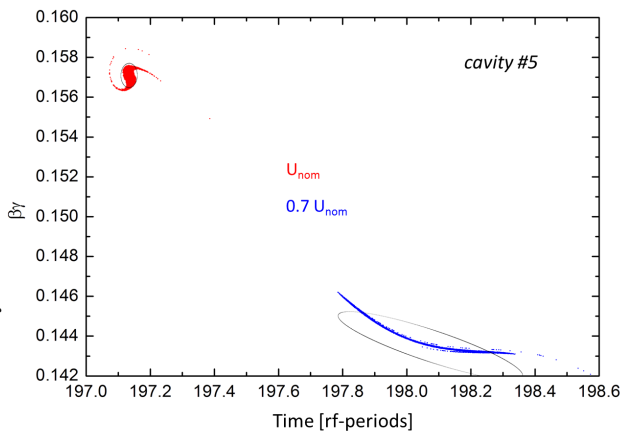


Figure 4: Longitudinal phase space distributions at the exit of the DTL. Red: last DTL cavity operated at nominal voltage. Blue: last cavity operated at 70% of the nominal voltage.

COMPLETE TRANSVERSE 4D BEAM DIAGNOSTICS

For any accelerator or transport lattice which includes elements coupling the transverse planes as solenoids for instance, complete 4d transverse beam diagnostics is required for adequate beam-based modeling of the lattice. The four 2nd order inter-plane correlations must be measured. To our knowledge such measurements never were conducted successfully before at ion energies beyond about 150 keV/u. Applying a slit/grid emittance meter preceded by a skewed quadrupole triplet such measurements were done with an uranium beam at 11.4 MeV/u. Details on this method can be found in [7].

Additionally, the ROTating System for Emittance measurements (ROSE) was developed and commissioned [8] with ⁸³Kr¹³⁺ beam at 1.4 MeV/u and with ²³⁸U²⁸⁺ beam at 5.9 MeV/u. It is a single-plane slit/grid emittance measurement device housed in a chamber which can be rotated around the beam axis (Fig. 5) by any angle θ . For one beam transport setting (a) emittance measurements were performed at rotation angles of 0°, 90°, and at an intermediate angle θ_0 . One additional measurement at θ_0 using a different setting (b) was done. The accuracy of the measured 2nd moments is sufficiently high to define transport sections that can completely decouple the beam with skewed quadrupoles for instance [8].

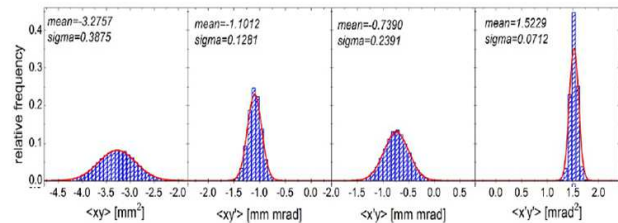
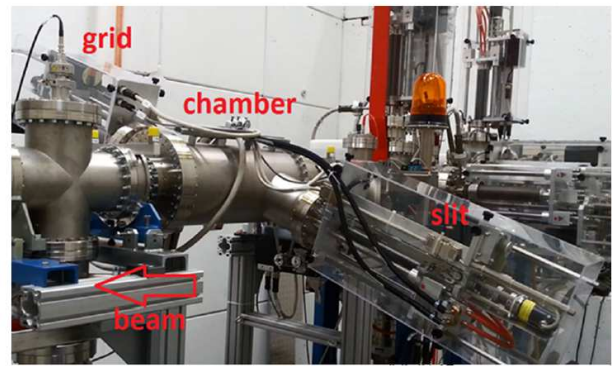


Figure 5: ROTating System for Emittance measurements ROSE (top). Measured 2nd order beam moments that quantify the amount of coupling between the horizontal and vertical plane (bottom).

EXTENSION OF THE BUSCH THEOREM TO BEAMS

In 1926 H. Busch formulated the preservation of the conjugated angular momentum of a single charge particle moving

along a region with longitudinal magnet field [9]. The generalization of the theorem [10] is expressed as

$$\oint_C \vec{v} \cdot d\vec{C} + \frac{eq}{m\gamma} \psi = const. \quad (5)$$

and visualized in Fig. 6. The path integral of the stream of possible particle velocities \vec{v} along a closed contour C confining a fixed set of possible particle trajectories, plus the magnetic flux through the area enclosed by C is an invariant of the motion.

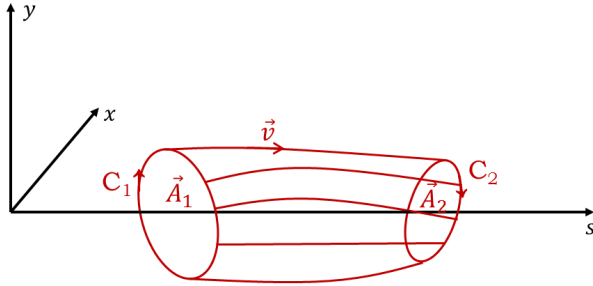


Figure 6: The contour C encloses possible streams of particle trajectories and encloses the area \vec{A} .

In 1992 A.J. Dragt introduced the eigen-emittances [11] as the rms-emittances $\varepsilon_{1/2}$ which the beam acquires after all of its inter-plane correlations have been removed. Accordingly, they are preserved by all linear elements even if they introduce correlations and change the rms-emittances. This section briefly summarizes the results and applications of extending Busch's theorem to accelerated particle beams [12]. The preservation of the sum of the squares of the two transverse eigen-emittances is expressed using conjugated variables. Finally, this preservation delivers a term that is quite similar to Eq. (5)

$$(\varepsilon_{n1} - \varepsilon_{n2})^2 + \frac{4eq\psi\beta\gamma}{m\pi} \oint_C \vec{r}' \cdot d\vec{C} + \left[\frac{eq\psi}{m\pi} \right]^2 = const., \quad (6)$$

where the integral is to be taken of the averaged beam divergence around the curve enclosing the beam rms-area divided by π . This expression connects the normalized eigen-emittances, the beam vorticity, and magnetic flux through the beam rms-area A . It turns out that this conservation law allows for very fast modeling of beam emittance shaping experiments done with electrons and with ions. In many cases application of conservation laws is more efficient w.r.t. solving the underlying equations of motion.

The first application is on Fermilab's flat beam experiment [13], where an electron beam was extracted from a cathode immersed into the magnetic flux B_0 (Fig. 7).

After acceleration to 16 MeV correlations were removed with skew quadrupoles. The final transverse emittance ratio is quickly derived using the extended Busch theorem by applying Eq. (6) at the cathode and at the exit of the beam

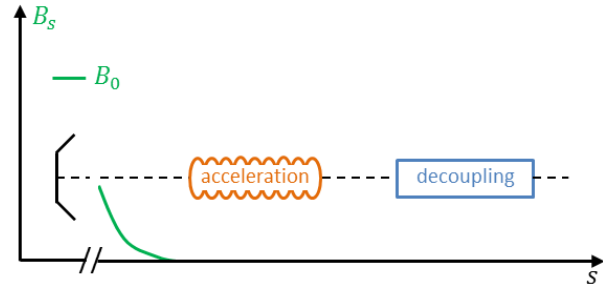


Figure 7: (from [12]) Schematic sketch of the beam line of the experiment performed at NICCAD at FERMILAB [13].

line

$$0 + 0 + \left[\frac{eB_0A_0}{mc} \right]^2 = (\varepsilon_{nf1} - \varepsilon_{nf2})^2 + 0 + 0, \quad (7)$$

which with few steps delivers the formula derived in [13]

$$\varepsilon_{nf1/2} = \pm \mathcal{L}\beta\gamma + \sqrt{(\mathcal{L}\beta\gamma)^2 + (\varepsilon_n'')^2}. \quad (8)$$

The second application is on the EMTEX experiment done at GSI [14,15] being sketched in Fig. 8. A beam of $^{14}\text{N}^{3+}$ was

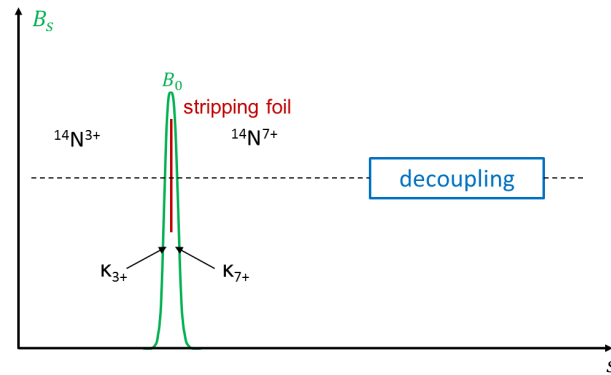


Figure 8: (from [12]) Schematic beam line of EMTEX at GSI for transverse emittance transfer [15].

passed through a solenoid with field B_0 into which charge state stripping to $^{14}\text{N}^{7+}$ was done. Accordingly, the fringe fields act differently on the beam at the solenoid entrance and exit, respectively. The imposed correlations were removed by a quadrupole triplet. The effective repartitioning of the emittances through EMTEX can be derived quickly from the extended Busch theorem. First it is applied to the entrance of the beam line and to the centre of the solenoid right before stripping as

$$\begin{aligned} & (\varepsilon_{x,3+} - \varepsilon_{y,3+})^2 + 0 + 0 \\ &= (\varepsilon_{1f} - \varepsilon_{2f})^2 + \frac{2B_0}{(B\rho)_{3+}} \mathcal{W}_{Af} + \left[\frac{A_f B_0}{(B\rho)_{3+}} \right]^2, \end{aligned} \quad (9)$$

where

$$\begin{aligned} \mathcal{W}_A &= 2A \oint_C \vec{r}'(x, y, s) \cdot d\vec{C} \\ &= \langle y^2 \rangle \langle xy' \rangle - \langle x^2 \rangle \langle yx' \rangle + \langle xy \rangle (\langle xx' \rangle - \langle yy' \rangle) \end{aligned} \quad (10)$$

Content from this work may be used under the terms of the CC BY 3.0 licence (© 2018). Any distribution of this work must maintain attribution to the author(s), title of the work, publisher, and DOI.

is twice the beam vorticity multiplied with the beam rms-area. Charge state stripping just changes the beam rigidity but does not change any other beam property (straggling and scattering can be neglected). Afterwards the invariance is re-formulated for the new charge state, i.e., at the centre of the solenoid right after stripping and at the exit of the beam line

$$(\varepsilon_{1f} - \varepsilon_{2f})^2 + \frac{2B_0}{(B\rho)_{7+}} \mathcal{W}_{Af} + \left[\frac{A_f B_0}{(B\rho)_{7+}} \right]^2, \quad (11)$$

$$= (\varepsilon_{x,7+} - \varepsilon_{y,7+})^2 + 0 + 0.$$

Combining these relationships leads to the final repartitioning of the projected beam rms-emittances

$$(\varepsilon_{x,7+} - \varepsilon_{y,7+})^2 = (\varepsilon_{x,3+} - \varepsilon_{y,3+})^2 + (A_f B_0)^2 \left[\frac{1}{(B\rho)_{7+}} - \frac{1}{(B\rho)_{3+}} \right]^2. \quad (12)$$

The equivalent deviation based on solving the equations of motion exceeds several pages [14].

OPTIMIZATION OF RING INJECTION WITH GENERIC ALGORITHM

The efficiency of injection from a linac into a circular accelerator depends on many parameters as position and angle of injected beam (x, x'), initial orbit bump x_b and its reduction rate T , number n of turns during injection, and the horizontal tune Q_x and emittance ε_x from the linac. Optimization of this parameter set was successfully done by applying a generic algorithm as reported in detail in [16]. A number of initial parameter sets is defined and labelled as initial generation. Their fitness w.r.t. efficiency is evaluated and the fittest are mixed pairwise to exchange single parameters combined with small mutations, i.e., arbitrary changes of single parameters. The new generation formed in that way is re-evaluated and the fittest are re-mixed partially with the previous generation to create the subsequent generation. Doing so, very fast convergence is achieved as depicted in Fig. 9 and the final result is much better compared to optimizations without generic algorithms.

The simulations of efficiency were benchmarked [17] with according measurements [18]. Using EMTEX the transverse emittance ratio was varied leaving all other beam parameters unchanged. Figure 10 plots the simulated and measured accumulation rates revealing excellent agreement.

REFERENCES

- [1] FAIR Baseline Technical Report, vol. 2, GSI Darmstadt, Germany, 2006, pp. 335.
- [2] P. Scharrer *et al.*, "Electron stripping of Bi ions using a modified 1.4 MeV/u gas stripper with pulsed gas injection", *J. Radioanal. Nucl. Chem.*, vol. 305, pp. 837-842 (2015), doi:10.1007/s10967-015-4036-2

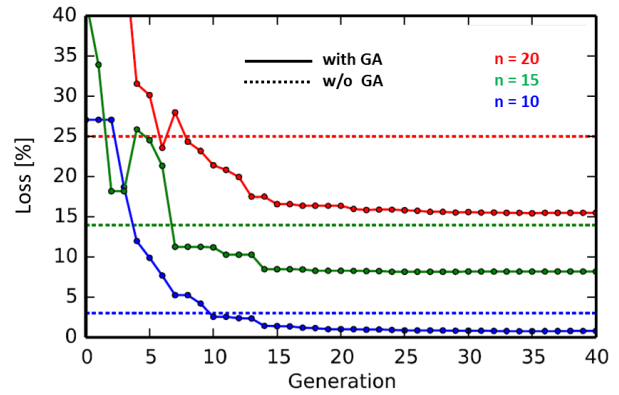
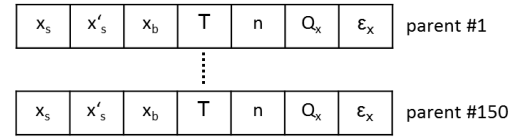


Figure 9: Solid lines: relative beam loss during multi-turn injection as a function of the generation comprising the parameter set used for the injection. Losses are plotted for different numbers of turns during injection. Dotted lines: Losses corresponding to injection parameter sets being obtained without applying generic algorithms.

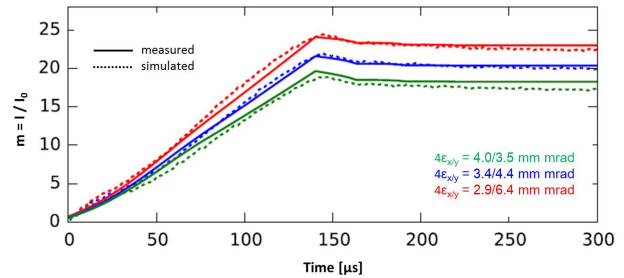


Figure 10: Measured (solid) and simulated (dotted) accumulated current during multi-turn injection as a function of time. Currents are plotted for different transverse emittance ratios provided by the linac through EMTEX.

- [3] P. Scharrer *et al.*, "Measurements of charge state distributions of 0.74 and 1.4 MeV/u heavy ions passing through dilute gases", *Phys. Rev. ST Accel. Beams*, vol. 20, pp. 043503 (2017), doi:10.1103/PhysRevAccelBeams.20.043503
- [4] U. Ratzinger, "The IH-Structure and its Capability to Accelerate High Current Beams", in *Proc. PAC 1991*, San Francisco, CA, USA, pp. 567.
- [5] C. Xiao *et al.*, "Investigations on KONUS beam dynamics using the pre-stripper drift tube linac at GSI", *Nucl. Instrum. Methods Phys. Res. A*, vol. 887, pp. 40 (2018), doi:10.1016/j.nima.2018.01.024
- [6] Y. K. Batygin *et al.*, "Particle-in-cell code BEAMPATH for beam dynamics simulations in linear accelerators and beam-lines", *Nucl. Instrum. Methods Phys. Res. A*, vol. 539, pp. 455 (2005), doi:10.1016/j.nima.2004.10.029
- [7] C. Xiao *et al.*, "Measurement of the transverse four-dimensional beam rms-emittance of an intense uranium beam

- at 11.4 MeV/u”, *Nucl. Instrum. Methods Phys. Res. A*, vol. 820, pp. 14 (2016), doi:10.1016/j.nima.2016.02.090
- [8] C. Xiao *et al.*, “Rotating system for four-dimensional transverse rms-emittance measurements”, *Phys. Rev. ST Accel. Beams*, vol. 19, pp. 072801 (2016), doi:10.1103/PhysRevAccelBeams.19.072802
- [9] H. Busch, “Berechnung der Bahn von Kathodenstrahlen im axialsymmetrischen elektromagnetischen Felde”, *Annalen der Physik*, vol. 81, pp. 974, (1926).
- [10] P. T. Kirstein *et al.*, *Space Charge Flow*. New York, USA: McGraw-Hill Inc., 1967, pp. 14.
- [11] A. J. Dragt, “General moment invariants for linear Hamiltonian systems”, *Phys. Rev. A*, vol. 45, no. 4, pp. 2572 (1992), doi:10.1103/PhysRevA.45.2572
- [12] L. Groening *et al.*, “Extension of Busch’s theorem to particle beams”, *Phys. Rev. ST Accel. Beams*, vol. 21, pp. 014201 (2018), doi:10.1103/PhysRevAccelBeams.21.014201
- [13] P. Piot *et al.*, “Photoinjector generation of a flat electron beam with transverse emittance ratio of 100”, *Phys. Rev. ST Accel. Beams*, vol. 9, pp. 031001 (2006), doi:10.1103/PhysRevSTAB.9.031001
- [14] C. Xiao *et al.*, “Single-knob beam line for transverse emittance partitioning”, *Phys. Rev. ST Accel. Beams*, vol. 16, pp. 044201 (2013), doi:10.1103/PhysRevSTAB.16.044201
- [15] L. Groening *et al.*, “Experimental Proof of Adjustable Single-Knob Ion Beam Emittance Partitioning”, *Phys. Rev. Lett.*, vol. 113, pp. 264802 (2014), doi:10.1103/PhysRevLett.113.264802
- [16] S. Appel *et al.*, “Injection optimization in a heavy-ion synchrotron using genetic algorithms”, *Nucl. Instrum. Methods Phys. Res. A*, vol. 852, pp. 73 (2017), doi:10.1016/j.nima.2016.11.069
- [17] S. Appel *et al.*, “Injection optimization through generation of flat ion beams”, *Nucl. Instrum. Methods Phys. Res. A*, vol. 866, pp. 6 (2017), doi:10.1016/j.nima.2017.05.041
- [18] L. Groening *et al.*, in *Proc. of IPAC 2015*, Richmond, VA, USA, 2015, pp. 153–155, doi:10.18429/JACoW-IPAC2015-MOPWA026